Dynamic response of a nonlinear parametrically excited system subject to harmonic base excitation

Bahareh Zaghari, Emiliano Rustighi and Maryam Ghandchi Tehrani
University of Southampton, Highfield Campus, Southampton, UK
E-mail: b.zaghari@soton.ac.uk

Abstract. A Nonlinear Parametrically Excited (NPE) system subjected to a harmonic base excitation is presented. Parametric amplification, which is the process of amplifying the system's response with a parametric excitation, has been observed in mechanical and electrical systems. This paper includes an introduction to the equation of motion of interest, a brief analysis of the equations nonlinear response, and numerical results. The present work describes the effect of cubic stiffness nonlinearity, cubic parametric nonlinearity, and the relative phase between the base excitation and parametric excitation under parametric amplification. The nonlinearities investigated in this paper are generated by an electromagnetic system. These nonlinearities were found both experimentally and analytically in previous work [1]; however, their effect on a base excited NPE is demonstrated in the scope of this paper. This work has application in parametric amplification for systems, which are affected by strong stiffness nonlinearities and excited by harmonic motion. A careful selection of system parameters, such as relative phase and cubic parametric nonlinearity can result in significant parametric amplification, and prevent the jump from upper stable solutions to the lower stable solutions.

1. Introduction

Parametrically excited oscillators and actuators have been introduced recently to amplify [2], suppress [3] or control [4] the response amplitude. Linear Parametrically Excited (LPE) systems, where defining system parameters vary with an independent variable (time), are a well-established concept in the field of electrical and mechanical engineering [5]. However, less attention has been dedicated to Nonlinear Parametrically Excited (NPE) systems as a result of their complexity in analytical and experimental studies. Real systems are nonlinear, and linearising systems with strong nonlinearity means essential information is lost [6]. For example, some nonlinearities in signal amplifiers improve their performance. Designing a low-noise signal amplifier for electronic devices is essential. Electromechanical parametric amplifiers have been introduced to address the above issue for micro/nano systems [7]. Traditionally, these amplifiers are operated in a linear range, however driving these amplifiers within a nonlinear frequency response regime can be beneficial. Rhoads et, al. [8] have shown the effect of hardening nonlinearity on a classical degenerate parametric amplifier (where the parametric frequency is locked at twice the frequency of the external signal). They evaluated the gain of the amplifier due to the effect of hardening nonlinearity for different parametric amplitude and phase between the direct excitation and parametric excitation. Gain is defined as a relation between the amplitude of response without parametric excitation and when parametric amplification is applied [8]. Recently, Neumeyer et, al. [9] investigated the effect of frequency detuning of parametric and

direct excitation for near resonant nonlinear systems. They showed, for some frequency ranges, frequency detuning might increase the steady-state response. This work is relevant to studies where frequency detuning can be expected between the parametric and direct excitation, or between the parametric and direct excitation and the system's natural frequency during system operation. Rhoads et, al. [10] demonstrated the potential of parametric amplification in a macro-scale mechanical amplifier. They used a cantilever beam under longitudinal and transverse base excitation as an example of a parametric amplifier. They found parametric amplification achieved a gain increase of a factor between $1.4-1.6$ when put into practice. Careful selection of phase can also cause response reduction, which can be used in other applications like vibration absorbers. Parametric amplification in the model presented by Rhoads et. al. occurred as a result of exciting the cantilever beam at twice its natural frequency with an angle with its motion. This model only could be used for checking the effect of parametric amplification on the gain, however the nonlinearities in the system could not be controlled, and their effect could not be examined separately. In this paper, the effect of parametric amplitude and parametric nonlinearities on the steady-state response is shown analytically. The experimental set-up is shown as motivation for future study on base excitation response of NPE systems. The relative phase between the base excitation and parametric excitation for each stable and unstable branches of solutions are examined, it is found the change in relative phase, amplify or suppress the response amplitude of each stable branches differently.

2. Methodology

The system of interest is a cantilever beam under transverse base excitation (figure 1). The base excitation is in the form of translation in the transverse direction with a small rotation (rotational motion is neglected in this study). Parametric excitation is introduced by a time-varying electromagnetic force on the cantilever beam. The electromagnetic force is generated by a set of coils and magnets when DC/AC current is carried by coils. This configuration is explained in previous work [1]. Here, a SDOF model is used to analyse the cantilever beam motion. The SDOF system parameters are defined as: x is the displacement of moving mass m_{h}, and Y_0 is the amplitude of harmonic base displacement at frequency ω and phase ϕ. The relative displacement z, is the displacement between the mass and base. The overall damping coefficient $c_{\mathrm{h}} = c_{\mathrm{m}} + c_{\mathrm{e}}$, where c_{m} and c_{e} are components due to mechanical and electrical damping respectively. The electrical damping c_{e} represents an electrical load from the electromagnetic system.

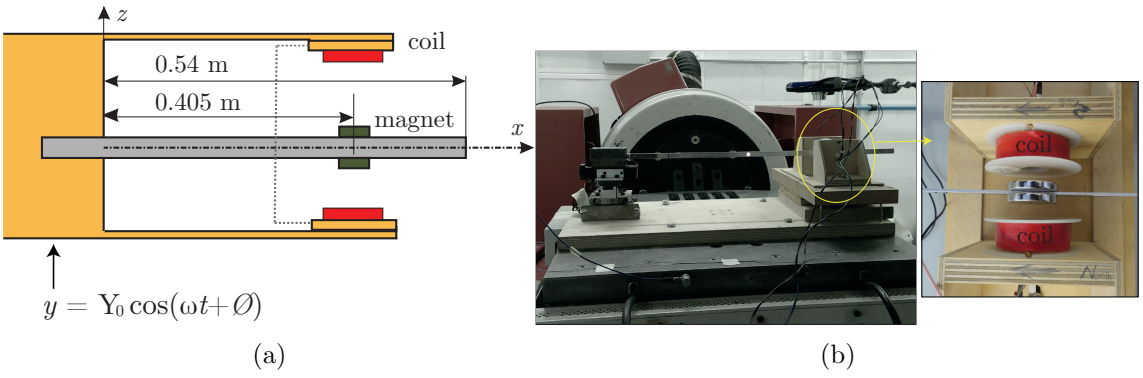

(a) (b)

Figure 1: (a) Schematic model of a cantilever beam under transverse base excitation. (b) Experimental set-up consisting of a cantilever beam on a shaker and electromagnetic system.

The governing differential equation of motion for the SDOF system is defined as:

$$m_{\mathrm{h}}\ddot{x} + \varepsilon c_{\mathrm{h}}(\dot{x} - \dot{y}) + \varepsilon k_{\mathrm{b}}(x - y) + \varepsilon F_{\mathrm{e}} = 0, \tag{1}$$

where k_{b} is the static stiffness of the cantilever beam before applying the electromagnetic force F_{e}, and ε is the small bookkeeping parameter introduced to facilitate analysis. The system parameters, m_{h}, c_{h}, and k_{b} are the physical parameters. Rearranging Eq. (1) in terms of the relative displacement of the mass $z = x - y$ yields

$$m_{\mathrm{h}}\ddot{z} + \varepsilon c_{\mathrm{h}}\dot{z} + k_{\mathrm{b}}z + \varepsilon F_{\mathrm{e}} = -\varepsilon m_{\mathrm{h}}\ddot{y}. \tag{2}$$

When base excitation is $y = Y_0\cos(\omega t + \phi)$, Eq. (2) is

$$m_{\mathrm{h}}\ddot{z} + \varepsilon c_{\mathrm{h}}\dot{z} + k_{\mathrm{b}}z + \varepsilon F_{\mathrm{e}} = \varepsilon m_{\mathrm{h}}\omega^2 Y_0\cos(\omega t + \phi). \tag{3}$$

The electromagnetic force F_{e} is modeled based on previous work [1]:

$$F_{\mathrm{e}}(t) = k_{\mathrm{ext}}z + k_{\mathrm{p1}}\cos(\Omega t)z + k_3 z^3 + k_{\mathrm{p3}}\cos(\Omega t)z^3 \tag{4}$$

where k_{ext} is the linear external stiffness due to the static electromagnetic force, k_{p1} is the time-varying stiffness with frequency Ω, k_3 is the cubic stiffness and k_{p3} is the cubic parametric stiffness as a result of nonlinearity in electromagnetic system.

The magnetic field produced by two current carrying coils and two magnets can be calculated assuming that the coils are perfect and have identical solenoids and that the magnets constitute a magnetic dipole. If the magnets and coils are repulsive, the magnets return to their equilibrium position, however when the magnets are not in the equilibrium position (z is the magnet displacement with respect to the equilibrium position) a force is generated from one set of current carrying coils is greater than the other one. When the coils are carrying a DC current the magnets are under the constant force and they are forced to stay at equilibrium position. When the coils are carrying an AC current as well as a DC current, the force on magnets will change with time, as a result of the change in the magnetic field with the frequency of AC current but still the magnets are positioned at the equilibrium position. In this work the current carried in coils has low frequency (less than 20 Hz), hence the coils inductance is neglected and only modeled as a resistor. Coils are connected in series. Repulsion effects of the electromagnetic force increase the stiffness of the cantilever beam, which manifests as hardening nonlinearity. Eq. (3) is normalised by the mass m_{h} and time scaling $\tau = \Omega t$, and is expressed as derivatives with respect to τ instead of t. Prime $(.)'$ represents a quantity differentiated with respect to τ. Normalisation in this way results in

$$z'' + \frac{2\varepsilon\zeta\omega_n}{\Omega}z' + \frac{\omega_n^2}{\Omega^2}(1 + \varepsilon\delta\cos(\tau))z + \frac{\omega_n^2}{\Omega^2}(\varepsilon\alpha + \varepsilon\gamma\cos(\tau))z^3 = \frac{1}{4}\varepsilon Y_0\cos(\frac{\tau}{2} + \phi). \tag{5}$$

Note that base excitation frequency ω is considered to be half of the parametric frequency $\omega = \frac{\Omega}{2}$. In this case, when $\Omega = 2\omega_{\mathrm{n}}$, only the response at the linear resonance frequency is considered. $\omega_n = \sqrt{\frac{k_1}{m_{\mathrm{h}}}}$ is the linear resonance frequency (first mode of the cantilever beam), k_1 is the total static stiffness $k_1 = k_{\mathrm{b}} + k_{\mathrm{ext}}$, ζ is the damping ratio, $\delta = \frac{k_{\mathrm{p1}}}{k_1}$, $\alpha = \frac{k_3}{k_1}$, $\gamma = \frac{k_{\mathrm{p3}}}{k_1}$, and ϕ is the phase between the parametric stiffness and base excitation. The averaging method is applied to solve Eq. (5). To capture the system's near-resonance behaviour, the parametric frequency Ω varies around the reference frequency Ω_0; thus Δ the detuning parameter is introduced as $\Omega = \Omega_0(1 - \varepsilon\Delta)$. If $\varepsilon = 0$, when the system is simplified to an undamped oscillator, the solutions of Eq. (5) are a linear combination of $\cos(\tau)$ and $\sin(\tau)$. This linear combination can

be written as $z(\tau) = a\cos(\kappa\tau + \varphi)$, where a and φ are the constant amplitude and the phase which can be determined from initial conditions. The frequency relation $\frac{\omega_n}{\Omega_0} = \kappa$ is used here for simplification. If $\varepsilon \neq 0$ is based on the "variation of constant" method of Lagrange, we can assume that the solution can still be written in the above form, but the amplitude and phase a and φ are now functions of time [11]. Hence, the complementary solution of the final simplified nonlinear equation (Eq. (5)) is a linear combination of $\cos(\Phi(\tau))$ and $\sin(\Phi(\tau))$, which can be written as $z(\tau) = a(\tau)\cos(\Phi(\tau))$, where $\Phi(\tau) = \kappa\tau + \varphi(\tau)$, and

$$z(\tau)' = a'(\tau)\cos(\Phi(\tau)) - a(\tau)(\kappa + \varphi'(\tau))\sin(\Phi(\tau)). \tag{6}$$

Substituting $\Phi(\tau)$ and Eq. (6) into Eq. (5) results an equation which can be solved for $a'(\tau)$ and $\varphi'(\tau)$. $\overline{a}'(\tau)$ and $\overline{\varphi}'(\tau)$ are averaged by assuming $a(\tau)$ and $\varphi(\tau)$ are changing slowly. $\overline{a}'(\tau)$ and $\overline{\varphi}'(\tau)$ are averaged over one period $T = \frac{2\pi}{\Omega}$. The resulting averaged equation can be integrated with respect to τ to find the $\overline{a}(\tau)$ and $\overline{\varphi}(\tau)$ for a given κ and reference frequency Ω_0. The steady-state behaviour of the system can be recovered from the set of $\overline{a}'(\tau)$ and $\overline{\varphi}'(\tau)$ by setting $(\overline{a}', \overline{\varphi}') = (0, 0)$ and solving for steady-state values of $\overline{a}$ and $\overline{\varphi}$:

$$\overline{a}'(\tau) = -\varepsilon\zeta\frac{\omega_n}{\Omega}\overline{a} + \varepsilon\frac{1}{8}\delta\sin(2\overline{\varphi})\overline{a} + \varepsilon\frac{1}{16}\gamma\sin(2\overline{\varphi})\overline{a}^3 + \varepsilon\frac{1}{4}Y_0\frac{\Omega^2}{\omega_n^2}\sin(\phi - \overline{\varphi}) \tag{7}$$

$$\overline{\varphi}'(\tau) = 0.5\varepsilon\Delta\overline{a} + \varepsilon\frac{1}{8}\delta\cos(2\overline{\varphi}) + \varepsilon\frac{1}{16}\alpha\overline{a}^2 + \varepsilon\frac{1}{8}\gamma\overline{a}^2\cos(2\overline{\varphi}) - \varepsilon\frac{3}{16}\frac{\Omega^2}{\omega_n^2\overline{a}}\cos(\phi - \overline{\varphi}). \tag{8}$$

The resulting solution is an approximation of the original solution:

$$\overline{a} = \frac{\Omega^2 Y_0\sqrt{(-p_1\sin(2\phi) + \zeta)^2 + (p_2 - p_3\cos(2\phi))^2}}{8\omega_n^2\left(p_1^2(1 - \cos(2\phi)^2) + p_3^2\cos(2\phi)^2 - p_2^2 - \zeta^2\right)}, \tag{9}$$

where $p_1 = \frac{1}{4}\left(\delta + \frac{1}{2}\gamma\overline{a}^2\right)$, $p_2 = \frac{3}{8}\alpha\overline{a}^2 - \frac{\Omega}{2\omega_n} + 1$, and $p_3 = \frac{1}{4}\left(\delta + \gamma\overline{a}^2\right)$. $\overline{a}$ represents the steady-state amplitude of non-trivial solutions. Eq. (5) has at least five stable and unstable non-trivial solutions when the system parameters δ, α, γ, $\psi \neq 0$.

3. The effects of parametric excitation and nonlinearities

The effect of parametric excitation for linear and nonlinear base excited systems is studied here. Several cases are introduced in table 1. A linear base excited system, Case A, is shown as a reference. A Linear Parametrically Excited (LPE) system, Case B, shows the parametric amplification caused by parametric excitation. A system with duffing nonlinearity is shown in Cases C and D, where both parametric excitation and duffing nonlinearity are considered. The transition curve for each cases are explained along with the amplitude-frequency curves (See figure 2). The effect of positive and negative cubic parameteric nonlinearity for a system with hardening nonlinearity and parametric excitation is investigated in Cases E and F.

When a linear non-parametric SDOF is considered ($\delta = \alpha = \gamma = \phi = 0$ in Eq. 5), the maximum amplitude is expected when base excitation frequency is equal to the natural frequency ω_n. Figure 3(a), shows the amplitude frequency plot (see Case A in table 1).

Case B is a LPE system when the electromagnetic force varies in time, and in this analysis the nonlinearities in the electromagnetic system are neglected. The steady-state amplitude of non-trivial solutions of the LPE system (Case B in table 1) from Eq. (9) are simplified to:

$$\overline{a} = \frac{\Omega^2 Y0\sqrt{\left(-\frac{1}{4}\delta\sin(2\phi) + \zeta\right)^2 + \left(1 - \frac{\Omega}{2\omega_n} - \frac{1}{4}\delta\cos(2\phi)\right)^2}}{\omega_n^2\left(2\frac{\Omega^2}{{\omega_n}^2} - \frac{1}{2}\delta^2 + 8\zeta^2 - 8\frac{\Omega}{\omega_n} + 8\right)}. \tag{10}$$

Table 1: Linear and nonlinear system parameters

	δ	α (m^{-2})	γ (m^{-2})	ζ	Y0 (m)	ϕ(rad)
Case A: Linear system	0	0	0	0.001	0.001	0
Case B: LPE system	0.1	0	0	0.001	0.001	$\frac{\pi}{2}$
Case C: Nonlinear system	0.001	1000	0	0.001	0.001	0
Case D: NPE system	0.1	1000	0	0.001	0.001	$\frac{\pi}{2}$
Case E: NPE system	0.1	1000	300	0.001	0.001	$\frac{\pi}{2}$
Case F: NPE system	0.1	1000	-300	0.001	0.001	$\frac{\pi}{2}$

The steady-state solutions are only found in the vicinity of parametric resonance outside the tongues in transition curves. The transition curves define the regions where the amplitude of the response is increased as a result of parametric excitation (inside the tongues) without the base excitation effect ($Y_0 = 0$). When parametric amplification is seen in linear systems, exponentially growing responses are expected inside the tongues [12]. Note that the denominator of Eq. (10) is zero when $\frac{\Omega}{\omega_n} = 2 \pm \frac{1}{2}\sqrt{\delta^2 - 16\zeta^2}$. Hence, unbounded solutions exist when

$$2 - \frac{1}{2}\sqrt{\delta^2 - 16\zeta^2} < \frac{\Omega}{\omega_n} < 2 + \frac{1}{2}\sqrt{\delta^2 - 16\zeta^2}. \tag{11}$$

Case B in table 1 is studied for a linear parametrically excited system, and the amplitude frequency relation plot is presented analytically and numerically in figure 3(b). Figure 3(b) shows that the steady-state amplitude increases close to parametric resonance, and that exponentially growing solutions are calculated numerically for $1.95 < \frac{\Omega}{\omega_n} < 2.05$. Also from figure 2, for Case B, $1.95 < \frac{\Omega}{\omega_n} < 2.05$ shows the region inside the instability tongue.

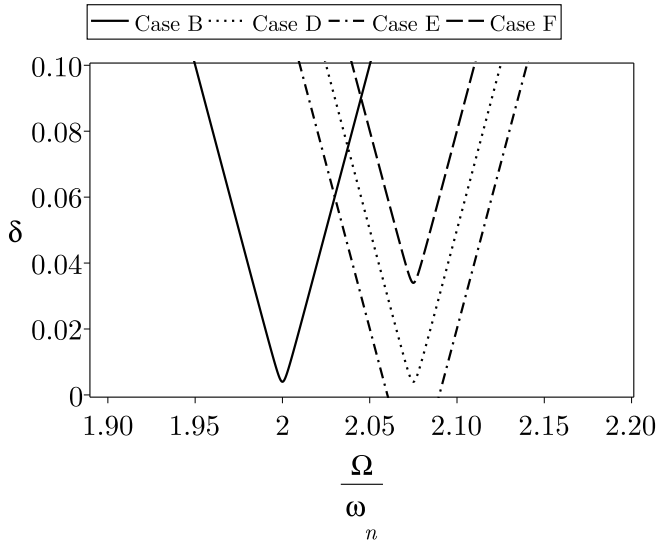

Figure 2: Linear transition curve corresponding to Case B and nonlinear transition curves corresponding to Cases D, E, and F for a given parametric amplitude δ. Since the transition curves for NPE systems are dependent on the amplitude of the steady-state response, in this plot the amplitude $\overline{a} = 0.01$(m) is kept constant. These cases are explained in table 1.

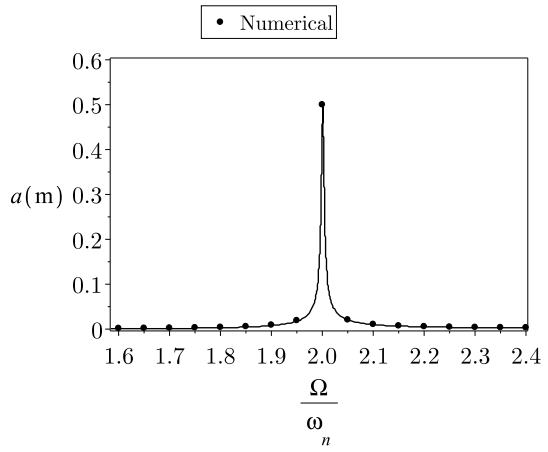

(a) Case A

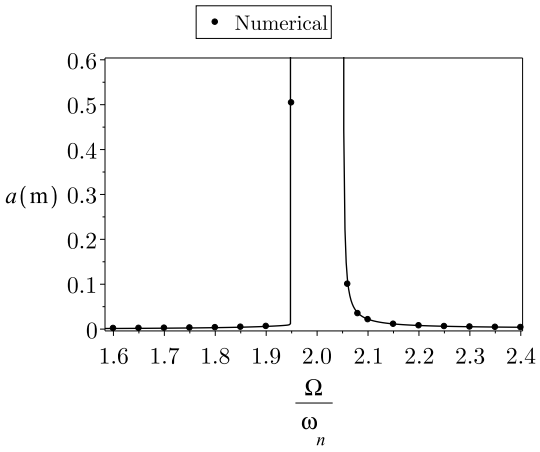

(b) Case B

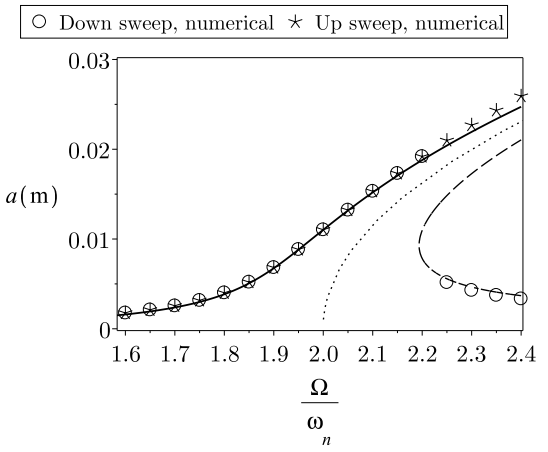

(c) Case C

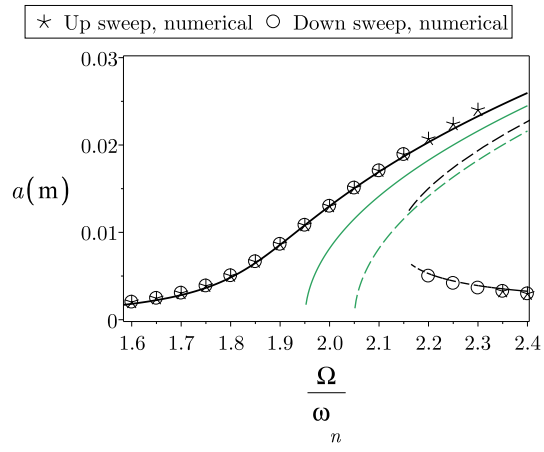

(d) Case D

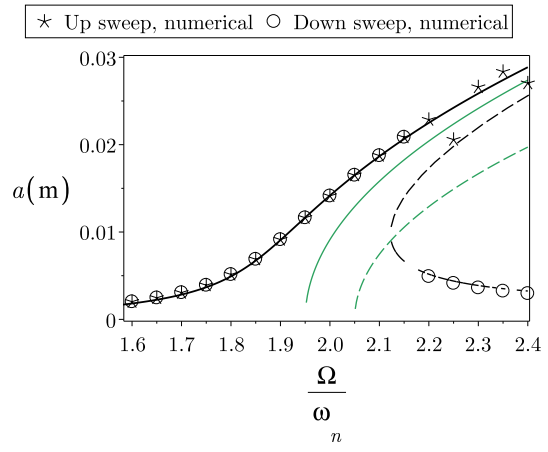

(e) Case E

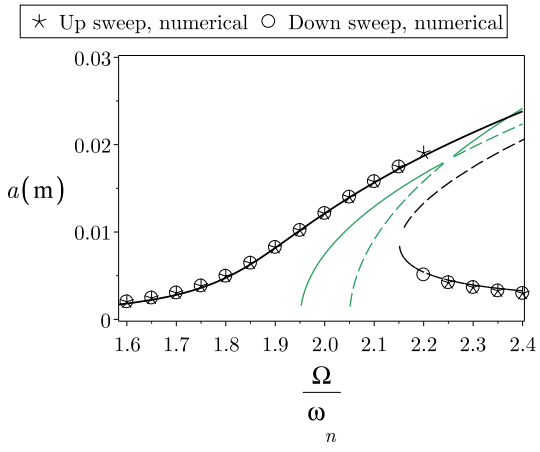

(f) Case F

Figure 3: Amplitude frequency relation, $\overline{a}$ versus $\frac{\Omega}{\omega_n}$ for Cases in table 1. These systems are solved analytically using the averaging method $(-)$, and direct numerical integration. (c) line presented by (....) is the *backbone curve*. For (d), (e) and (f), black lines represent solutions produced by base and parametric excitation, and the green lines represent solutions affected only by parametric excitation.

A harmonically excited duffing oscillator (when $\delta = \gamma = \phi = 0$ in Eq. (5)), has been studied in literature [13]. The effect of hardening ($\alpha > 0$) and softening ($\alpha < 0$) nonlinearities have also been studied [13]. Case C in table 1 investigates the effect of adding parametric amplitude below its parametric instability ($\delta < 4\zeta$) with hardening nonlinearity. Figure 3(c) shows the frequency response plot for Case C, where three branches of solutions are present. These solutions can be found from Eq. (9) by solving it for $\overline{a}$. Solid lines represent stable solution branches, and dashed lines represent unstable solution branches. A good agreement between the theoretical predictions and direct numerical integration is shown. A *backbone curve* corresponds to the solution of the nonlinear system on the hypothesis that both forcing and damping are null, or equivalently, that the base excitation compensates the damping forces in the system at those particular frequencies and amplitudes. A *backbone curve* is found for $\gamma = \zeta = \phi = 0$, when the parametric amplitude is considered as an external force on the system that affects the *backbone curve*:

$$\frac{1}{16}\delta^2 - (\frac{3}{8}\alpha\overline{a}^2 - (\frac{\Omega}{2\omega_n} - 1))^2 = 0. \tag{12}$$

A NPE system, Case D, is driven near parametric resonance above the parametric instability, where $\delta > 4\zeta$ (see table 1). In this case strong hardening nonlinearity is applied since the electromagnetic system is in repulsion. Though only responses with hardening nonlinearity are presented here, softening nonlinearities, like ($\alpha < 0$) behaviours, could not be easily achieved. When the electromagnetic system is in attraction, due to strong attraction forces, it is difficult to maintain the equilibrium state.

Case D features five distinct response branches. The two additional branches present compared to Case C arise from the coexistence of two resonances within the nonlinear parametric system. One resonance is induced by combination of base and parametric excitation, and the other is caused by parametric excitation. In this paper, we refer to stable and unstable branches caused only by parametric excitation as "additional branches". In figure 3(d), the additional branches are shown in green and other stable and unstable branches are presented in black. In figure 3(d) the solid lines are the stable branches and the dashed lines are the unstable branches. The two additional branches are comparable in magnitude to the other stable/unstable branch pair. The stable/unstable branches produced as a result of parametric excitation and base excitation, they are dependent on base excitation amplitude and parametric amplitude, however the additional branches only alter when the parametric amplitude is varied.

The transition curves are independent of base excitation amplitude and are dependent on the amplitude of the response for NPE systems. Figure 2 shows the transition curve for Case D when $\overline{a} = 0.01(m)$. For NPE systems the transition curves define the regions which for a given amplitude of response, additional stable and unstable solution branches exist. The transition curve for the NPE system is also shifted to the right as a result of positive cubic nonlinearity.

The effect of positive cubic parametric nonlinearity on a NPE system driven near parametric resonance above the parametric instability is considered (Case E in table 1). Cubic parametric nonlinearity increases the amplitude of the steady-state response. Both upper stable branches in figure 3(e) have been increased as a result of positive cubic parametric nonlinearity, compared to figure 3(d) when cubic parametric nonlinearity was considered equal to zero. Additional stable and unstable branches separate from each other at higher amplitude and frequency since the transition curve for a given system is expanded. Figure 2 shows the transition curve for Case E when the response amplitude is $\overline{a} = 0.01(m)$. At $\delta = 0.1$ the transition curve for Case E is larger than the transition curve for Case D, which shows the stable and unstable additional branches for Case E have larger separation compared to the stable and unstable additional branches for Case D. However, if negative cubic parametric nonlinearity is applied (Case F), the amplitude of the steady-state response will be decreased. Figure 3(f) shows the effect of negative cubic parametric nonlinearity on upper stable branches. This also can be seen in the transition curve

plot, figure 2 for Case F, when the transition curve is shifted up compare to the transition curve for Cases D and E, where higher cubic parametric nonlinearity was applied. At $\delta = 0.1$ the transition curve for Case F has the smallest region compared to Cases D and E. This is in agreement with figure 3(f), when the additional stable and unstable branches are closer together when compared to Cases D and E in Figs 3(d) and (e).

4. The effects of phase

The gain associated with the linear PE system, introduced in the previous section can be defined as

$$\text{Gain} = \frac{\overline{a}\,|_{\delta\neq 0}}{\overline{a}\,|_{\delta,\alpha,\gamma\neq 0}}. \tag{13}$$

Gain is calculated from Eq. (9) from the amplitude of the steady-state response when $\alpha = \gamma = 0$ and $\delta \neq 0$ over the amplitude of the response for a linear system ($\delta = \alpha = \gamma = 0$). This metric shows the value of parametric amplitude δ or relative phase ϕ for which the LPE system has higher response amplitude compared to a linear nonparametric system.

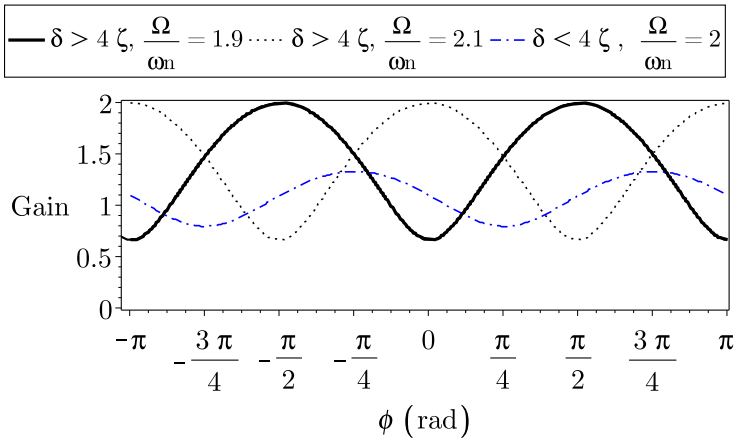

Figure 4: Gain versus phase ϕ for a LPE system.

The gain depends on relative phase ϕ. Figure 4 presents the effect of varying relative phase on gain. The maximum gain is found when $\phi = \frac{\pi}{2}$(rad) with the parametric amplitude above its parametric instability $\delta > 4\zeta$, however when the parametric amplitude is chosen under the parametric instability $\delta < 4\zeta$ the maximum gain is achieved at $\phi = \frac{3\pi}{4}$(rad). The phase relationship is repeated on π (rad) intervals. When the LPE system is excited with parametric amplitude above its parametric instability at $\frac{\Omega}{\omega_n} = 2$, the gain grows exponentially since the response is unbounded (see figure 3 (b)). Hence, gain is calculated at $\frac{\Omega}{\omega_n} = 1.9$ when the steady-state response is bounded (see figure 3 (b)). When the LPE system is excited with parametric amplitude below its parametric instability ($\delta < 4\zeta$), it is possible to excite the system at $\frac{\Omega}{\omega_n} = 2$ since solutions are bounded in this region. From figure 3 (b), it is evident that for a LPE system excited above its parametric instability, at $\frac{\Omega}{\omega_n} = 1.9$ and $\frac{\Omega}{\omega_n} = 2.1$ the amplitude of the response ($\overline{a}$) is different. The stable branch at $\frac{\Omega}{\omega_n} = 1.9$ is known as the upper stable branch, and the lower stable branch is at $\frac{\Omega}{\omega_n} = 2.1$ [1]. These two stable branches are comparable in magnitude when LPE/NPE systems have different relative phase ϕ. In figure 4, when $\frac{\Omega}{\omega_n} = 2.1$ and parametric amplitude is above its parametric instability, the maximum gain occurs when the relative phase is $\phi = 0$(rad), and the minimum gain is found when relative phase is $\phi = \frac{\pi}{2}$(rad).

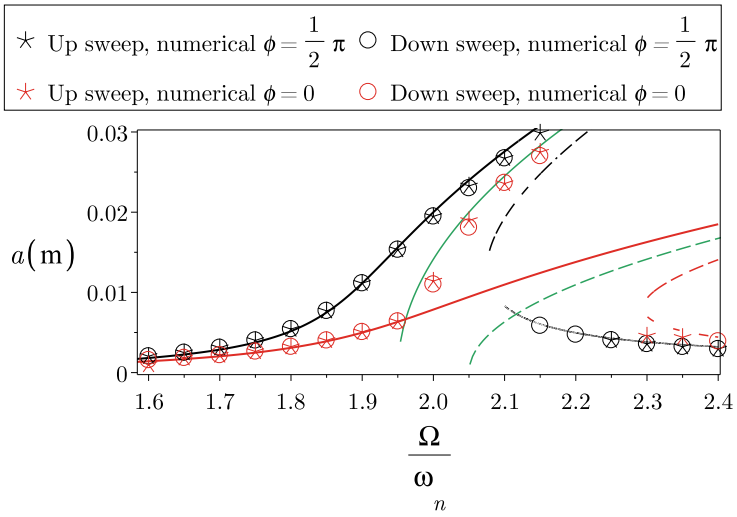

Figure 5: Amplitude frequency relation, $\overline{a}$ versus $\frac{\Omega}{\omega_n}$.

Stable and unstable solutions of the NPE system are affected by the relative phase between the base excitation and parametric excitation. Stable branches in figure 3 (shown with solid black lines) can be varied by the relative phase. The additional branches (green lines) are not affected by base excitation, hence they are independent of the phase between the base excitation and the parametric excitation.

Figure 5 shows the amplitude frequency relation for a NPE system with system parameters $\delta = 0.1$, $\alpha = 1000(\mathrm{m}^{-2})$, $\zeta = 0.001$, $Y_0 = 0.001(\mathrm{m})$ and when cubic parametric nonlinearity is a positive large value $\gamma = 1000(\mathrm{m}^{-2})$ for two different phases $\phi = \frac{\pi}{2}$ and $\phi = 0$ (rad). Black lines correspond to the analytical solutions when $\phi = \frac{\pi}{2}$ (rad) and red lines show the analytical solutions when $\phi = 0$ (rad). For both cases with different relative phase ϕ, the additional stable/unstable branches are fixed. The comparison between the amplitude of the response for these two phases shows that the upper branch is higher when $\phi = \frac{\pi}{2}$ (rad), however the lower branch is reduced compared to when $\phi = 0$ (rad). For a NPE system with $\phi = 0$ (rad), the upper stable branch (red line in figure 5) and the stable additional branch (green line in figure 5) are separated from each other, and as a result of this the jump phenomenon between these two branches are expected.

5. Conclusions

This work demonstrated the effect of electromechanical nonlinearities on the near-resonant response of a base-excited cantilever beam. The cantilever beam was excited by parametric excitation as well as the base excitation. The amplitude of response for linear and nonlinear parametrically excited systems was explained analytically for various system parameters with the averaging method and it was in agreement with the numerical integration. For a LPE system it was shown that the system has parametric amplification above its parametric instability, however adding the hardening nonlinearity reduces the response amplitude. The novel achievement of this work was related to the effect of relative phase on the different branch of solutions. It is possible to reduce and increase the amplitude of each stable branches by varying the relative phase. Stable branches were produced only because of the parametric amplification and they are not affected by the base excitation.

References

[1] Zaghari B, Rustighi E and Ghandchi Tehrani M 2015 An experimentally validated parametrically excited vibration energy harvester with time-varying stiffness *SPIE Smart Structures and Materials+ Nondestructive Evaluation and Health Monitoring* (International Society for Optics and Photonics) pp 94390S–94390S

[2] Zaghari B, Rustighi E and Ghandchi Tehrani M 2014 Experimental study on harvesting energy from a parametrically excited system *MoViC2014: The 12th International Conference on Motion and Vibration Control*

[3] Dohnal F and Mace B 2008 Amplification of damping of a cantilever beam by parametric excitation *Proceedings-CD MOVIC 2008* (Institute of Applied Mechanics)

[4] Ghandchi Tehrani M and Kalkowski M K 2015 *Journal of Intelligent Material Systems and Structures* 1045389X15588625

[5] Kovacic I and Cartmell M P August 2012 Special issue on parametric excitation: Applications in science and engineering *Proceedings of the Institution of Mechanical Engineers, Part C: Journal of Mechanical Engineering Science* pp 1909–1911

[6] Thomsen J J 2013 *Vibrations and stability: advanced theory, analysis, and tools* (Springer Science & Business Media)

[7] Rhoads J F and Shaw S W 2008 The effects of nonlinearity on parametric amplifiers *ASME 2008 International Design Engineering Technical Conferences and Computers and Information in Engineering Conference* (American Society of Mechanical Engineers) pp 593–597

[8] Rhoads J F and Shaw S W 2010 *Applied Physics Letters* **96** 234101

[9] Neumeyer S, Van Gastel M, Sorokin V and Thomsen J 2015 Frequency detuning effects for parametrically and directly excited elastic structures *Proceedings of 5th ECCOMAS Thematic Conference on Computational Methods in Structural Dynamics and Earthquake Engineering, May 2015* pp 1–7

[10] Rhoads J F, Miller N J, Shaw S W and Feeny B F 2008 *Journal of Vibration and Acoustics* **130** 061006

[11] Verhulst F 1996 *Nonlinear differential equations and dynamical systems* (Springer Science & Business Media)

[12] Cartmell M 1990 *Introduction to linear, parametric and nonlinear vibrations* (Chapman and Hall London)

[13] Kovacic I and Brennan M J 2011 *The Duffing equation: Nonlinear oscillators and their behaviour* (John Wiley & Sons)